

Journal of Materials Chemistry C

Accepted Manuscript



This is an *Accepted Manuscript*, which has been through the Royal Society of Chemistry peer review process and has been accepted for publication.

Accepted Manuscripts are published online shortly after acceptance, before technical editing, formatting and proof reading. Using this free service, authors can make their results available to the community, in citable form, before we publish the edited article. We will replace this *Accepted Manuscript* with the edited and formatted *Advance Article* as soon as it is available.

You can find more information about *Accepted Manuscripts* in the [Information for Authors](#).

Please note that technical editing may introduce minor changes to the text and/or graphics, which may alter content. The journal's standard [Terms & Conditions](#) and the [Ethical guidelines](#) still apply. In no event shall the Royal Society of Chemistry be held responsible for any errors or omissions in this *Accepted Manuscript* or any consequences arising from the use of any information it contains.

COMMUNICATION

High sensitive and selective formaldehyde gas sensor using molecular imprinting technique based on Ag-LaFeO₃†

Cite this: DOI: 10.1039/x0xx00000x

Received 00th January 2014,
Accepted 00th January 2014,

DOI: 10.1039/x0xx00000x

www.rsc.org/

Yumin Zhang^{ab}, Qingju Liu^{*a}, Jin Zhang^{ab}, Qin Zhu^{ab} and Zhongqi Zhu^{ab}

A novel formaldehyde gas sensor was developed for the first time using molecular imprinting technique (MIT) in semiconductor oxide to recognize small organic molecules. For the specific recognition, the as prepared molecular imprinting nanoparticles exhibit good selectivity for formaldehyde. Then the molecular imprinting nanoparticles were mixed with Ag-LaFeO₃ to form a compound. The compound with a small dimension and good dispersity possesses extremely high surface-to-volume ratio. Therefore the compound exhibits even better formaldehyde-sensing properties. At 40 °C, the response to 0.5 ppm formaldehyde based on the compound is 24.5, and lower than 3.0 to the other test gases. The response time and recovery time are 67 s and 104 s, respectively.

Formaldehyde is considered to be one of the most important industrial and commercial chemicals due to its chemical activity, high purity and relative cheapness.¹⁻³ It is well known that formaldehyde has been classified as a mutagen and possible human carcinogen by both the US Environmental Protection Agency (EPA) and the World Health Organization (WHO) for its toxin, anaphylaxis and accumulation.^{4, 5} So it is very necessary to monitor the formaldehyde in atmospheric environment quickly and accurately. Gas sensors based on semiconducting oxides are thought to be an effective means to monitor the gases because they are small, low cost and easy to use.^{6, 7} For the current contribution, lanthanum ferrite (LaFeO₃) has been selected because of its good thermostability,⁸ controllable structure,⁹ and our own experience in this field.^{10, 11}

The molecular imprinting method is a useful technique for preparing host polymers for molecular recognition. Various kinds of host polymers have been reported to have a high recognition property which is specific for imprinted template molecules.¹²⁻¹⁴ In this approach, the shape and functionality of a template can be transcribed onto microporous materials. The configuration of the

functional groups in the template may be memorized within the host polymers. Today, this field has become dominated by the use of organic polymeric materials for chromatographic separation, enzyme-mimicking catalysts, chemical sensors, and biosensors.¹⁵⁻²⁰

Song et al.²¹ designed ZnO-SnO₂ NTs with Ag NPs surface sensitization and carefully studied their enhanced sensing properties for low concentration (0.1 ppm) formaldehyde detection. Ding et al.²² reported for the first time that polyamide 6 (PA 6) NFN membranes were ESN deposited on QCM and employed as a unique platform to be functionalized with PEI molecules. The device exhibit good selectivity to formaldehyde. Lin et al.²³ prepared In₂O₃-sensitized flowerlike ZnO with visible light photoelectric response properties. The gas response to 5 ppm and 100 ppm formaldehyde can reach to 19% and 419% under visible light irradiation at room temperature, respectively. However, there is no report on using molecular imprinting technique in the field of gas sensor including formaldehyde gas sensor based on semiconducting oxides. Here, we report a formaldehyde gas sensor using MIT based on Ag-LaFeO₃ (1/99Ag-LaFeO₃ called Sample-A in the following text, details are illustrated in Experimental section) and also a compound composed of Sample-A and molecular imprinting nanoparticles (MINs) we prepared. These sensors show stronger response to formaldehyde gas. More importantly, they exhibit excellent selectivity to formaldehyde. Especially the compounds possess even better properties. At 40 °C, the response to 0.5 ppm formaldehyde based on the compound is 24.5, and to the other test gases the response are all lower than 3.0. The response time and recovery time are 67 s and 104 s, respectively.

Based on our previous work,¹⁰ the Sample Ag modified LaFeO₃ with Ag: La=1:99 mole ratio (called Sample-A, namely, Sample-A=1/99Ag-LaFeO₃) was found to be the most promising for the sensing properties to formaldehyde. In this study, the sol of Sample-A was used as crosslinker and further modified based on MIT.

Preparation of crosslinker: All the chemicals used are analytic grade reagents without further purifications from Tianjin Kermel Chemical Reagents Development Center. To prepare the crosslinker, 9.9 mmol $\text{La}(\text{NO}_3)_3 \cdot 6\text{H}_2\text{O}$, 10.0 mmol $\text{Fe}(\text{NO}_3)_3 \cdot 9\text{H}_2\text{O}$ and 10.0 mmol citrate were dissolved in 100 mL distilled water as solution A. 0.1 mmol AgNO_3 were dissolved in 10 mL distilled water and added to solution A drop by drop (12 drop/min), and then polyethylene glycol was added. The final mixed solution was kept stirring at 80°C for 8 h, and then was put in the microwave chemical device (CEM, USA) to synthesize at 75°C for 2 h, and the sol of Sample-A was formed, the sol was then used as crosslinker in the molecular imprinting process. The final sol was called solution B in the following text.

Preparation of MINs: To prepare MINs, formaldehyde used as template, acrylamide (AM) used as functional monomer, azodiisobutyronitrile (AIBN) used as initiator and solution B used as crosslinker. The molar ratio of template and functional monomer was defined as $x = \text{mol}(\text{formaldehyde}) : \text{mol}(\text{AM}) = 1:1, 1:2, 1:3$ and $1:4$. 1.0 mmol formaldehyde mixed with x mmol AM was treated by ultrasonic concussion for 30 min, and stand for 8 h as solution C. Then, 1.0 mmol AIBN was dissolved in 20 mL acetaldehyde and mixed with solution C and solution B. The final mixture was treated by ultrasonic concussion for 30 min, stirred at 50°C for 12 h with the protection of nitrogen and circulating water and then dried. Finally, the xerogel was heated at 800°C for 2 h. The MINs were finally prepared.

Preparation of the compound composed of Sample-A and the MINs with $x = 1:3$ (Sample-B): The weight ratio of Sample-A and Sample-B was defined as $a:b = w(\text{Sample-A}) : w(\text{Sample-B}) = 1:9, 3:7, 5:5, 7:3, 8.5:1.5, 9:1, 9.3:0.7, 9.5:0.5$ and $9.7:0.3$. 0.1a g Sample-A and 0.1b g Sample-B were mixed and added in 30 mL distilled water, treated by ultrasonic concussion for 30 min and put in the microwave chemical device to synthesize for 2 h and then dried. The compounds were finally prepared.

Fabrication of sensors: The prepared MINs and compounds were further mixed with distilled water respectively and ground to form a paste, which was subsequently printed onto an alumina tube. There are two Au electrodes placed at the both end sides of the tube (ESI, Fig. S1a-c). The length of the alumina tube is 4 mm and the diameter is 1.2 mm. In order to improve their stability and repeatability, the gas sensors were aged at 150°C for 170 h in air. The gas-sensing properties were test by WS-30A gas sensor tester (ESI, Fig. S1d-e).

Characterization: The X-ray Diffraction (XRD) patterns were obtained for the phase identification with a D/max23 diffractometer using $\text{Cu K}\alpha 1$ radiation ($\lambda = 1.54056 \text{ \AA}$), where the diffracted X-ray intensities were recorded as a function of 2θ . The accelerating voltage was 35 kV and the applied current was 25 mA, and the sample was scanned from 20° to 80° (2θ) in steps of 0.02° . The functional group was identified by fourier transform infrared spectrometer (FTIR, FTS-40) and the sample was scanned from 4000 cm^{-1} to 400 cm^{-1} with KBr pellet method. The particle morphology of the sample was tested by transmission electron microscope (TEM, JEM-2100). The particle size was attained through Nano-series Zeta Sizer.

Gas sensing properties of the MINs with $x=1:3$ (Sample-B) and the compounds with $a:b = 9:1$ (Sample-C) are better than those with $x=1:1, 1:2$ and $1:4$ and those with $a:b = 1:9, 3:7, 5:5, 7:3, 8.5:1.5, 9.3:0.7, 9.5:0.5$ and $9.7:0.3$, respectively (ESI, Fig. S2). So in this paper, we mainly discuss Sample-B and Sample-C.

X-ray powder diffraction patterns of MINs and compounds are showed in Fig. 1. The patterns in Fig. 1a indicate that the structure of MINs is orthogonal perovskite, which include only one phase of LaFeO_3 , this because the amount of Ag is so small ($\text{mol}(\text{Ag}) : \text{mol}(\text{LaFeO}_3) = 1\%$) that can't be detected and the template, functional monomer and initiator are removed after sintering, only some functional group left on the crosslinker,²⁴ which can't be detected either. Similar phenomena were also observed from the compound-based sensor in Fig.1b.

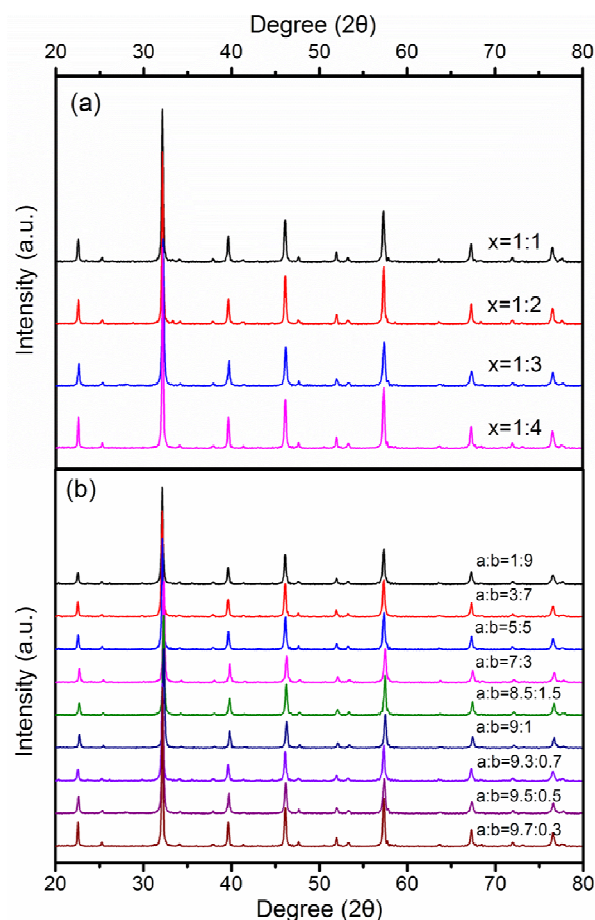


Fig. 1 XRD patterns of a) MINs ($1:4 \leq x \leq 1:1$) and b) compounds ($1:9 \leq a:b \leq 9.7:0.3$).

Fig. 2 shows the FT-IR spectroscopy of Sample-A, Sample-B and the functional monomer Acrylamide (AM). In the curve of Sample-A, the peaks around 565 cm^{-1} , 2341 cm^{-1} , 3485 cm^{-1} indicate Fe-O vibrations, the gas phase carbon dioxide vibrations and the stretching vibration of O-H²⁵ of H_2O in air respectively, and the peaks around 1412 cm^{-1} and 1582 cm^{-1} are attributed to the La-O vibrations.²⁶ In the curve of Sample-B, new peak at 1680 cm^{-1} has appeared compared with the curve of Sample-A, which is attributed to the stretching vibration of C=O in amidogen.²⁷ Compared the curves of Sample-B and AM, the weakening of the relatively strong peak of C=O stretching vibration (1680 cm^{-1}) and the disappearance

of N-H stretching vibration (3183 cm^{-1} and 3354 cm^{-1} ²⁷) in amidogen of Sample-B suggest the successful interaction between Ag-LaFeO₃ and AM, and the interaction should be ascribed to the coordination between amidogen groups in AM and La in Ag-LaFeO₃.²⁸

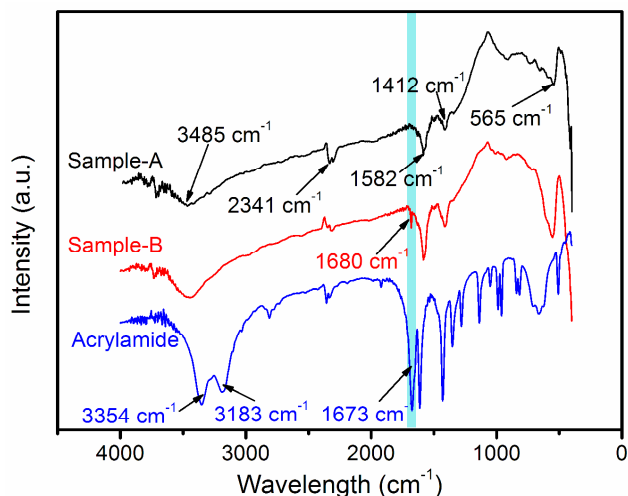


Fig. 2 Infrared spectra of sample-A, Sample-B and Acrylamide.

Transmission electron micrographs for the materials of Sample-B and Sample-C are shown in Fig. 3. For Sample-B (Fig. 3a), the particles are generally irregular and agglomerated, and the particle size was in the range of 60 nm-150 nm. While for Sample-C (Fig. 3b), there are many square-spherical shaped particles which are uniform in size and well dispersed, the particle size was in the range of 30 nm-70 nm. Thus the specific surface area of the compound is increased, which can adsorb formaldehyde more easily and enhance the response. The morphological features reveal that the particle size decreases with compounding with Sample-A.

The average particle size of Sample-B and the compounds are shown in Fig. 4. The width of the peak indicates the distribution of the particle size, namely, when the peak width is narrower, the particles are more uniform in size and better dispersed. As in Fig. 4, the average size of Sample-B and Sample-C are 190.7 nm and 44.9 nm, respectively. It indicates that the particles of Sample-B are agglomerated while the particles of Sample-C are well dispersed. Among all the compounds, the average particle size of Sample-C is smaller and more uniform than the others. For Sample-C, good dispersity and smallest particle size result in the largest surface area. The result is in accordance with that of TEM images.

LaFeO₃ is a typical p-type semiconductor in air, and its gas sensing mechanism is based on the changes of the resistance before and after being exposed to the test gas (ESI, Fig. S3).¹¹ After Ag-LaFeO₃ polymerized with AM, the gas sensing mechanism is similar to that of LaFeO₃, because LaFeO₃ is the only phase in MINs (Fig. 1, XRD patterns). The mechanism of the specific recognition of formaldehyde is illustrated in Fig. 5. A number of recognition cavities complementary to formaldehyde in shape, size and chemical functionality can selectively adsorb formaldehyde so the sensor

selectivity can be improved obviously. As illustrated by Fig. 5, when the template (formaldehyde) is mixed with functional monomers (AM), formaldehyde is allowed to interact via hydrogen-bond with AM, and then a formaldehyde-AM complex is formed.²⁴ The resulting complex is subsequently copolymerized with a large excess of crosslinker. Finally, after the removal of the template, recognition cavities complementary to formaldehyde molecules were formed on the surface of Ag-LaFeO₃, which have much accessible sites, high recognition and binding ability for formaldehyde and result in the improvement of the selectivity of the sensor. The thickness of the polymer layer on the nanoparticles is 4 nm-5 nm (Fig. 3b illustration). Inside of this layer, there are amounts of recognition cavities complementary to formaldehyde in shape, size and chemical functionality which can selectively adsorb formaldehyde. Among the test gases near the surface of sensing materials, only formaldehyde can be easily recognized and then react with the matrix Ag-LaFeO₃. This layer acts as a shield and only adsorbs the formaldehyde. So compared with Ag-LaFeO₃, MINs exhibit better selectivity meanwhile maintain the high response.

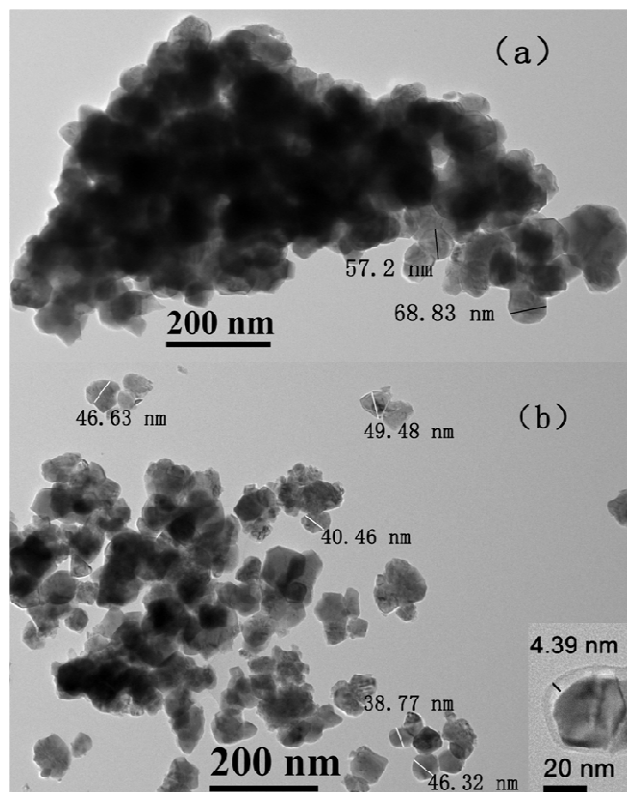


Fig. 3 TEM images of the materials of a) Sample-B and b) Sample-C.

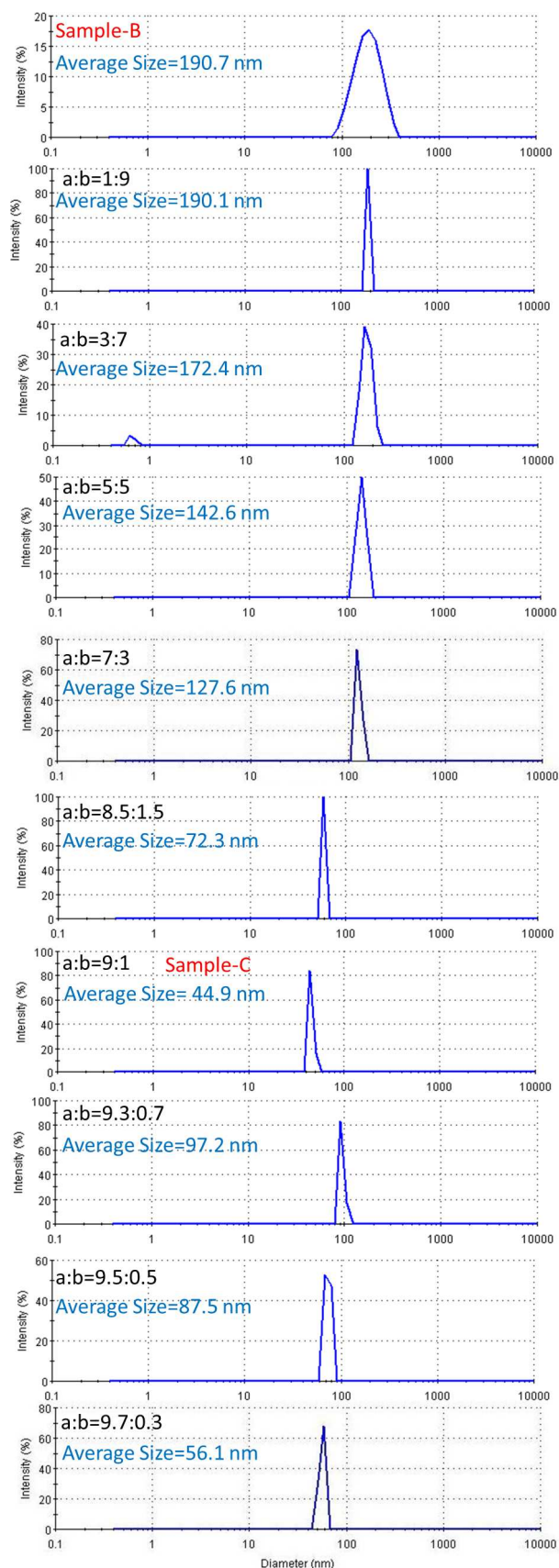


Fig. 4 Particle size of Sample-B and the compounds.

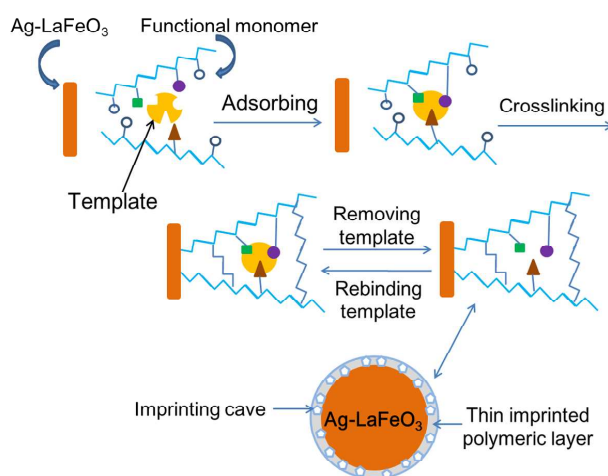


Fig. 5 Schematic diagram of molecular imprinting process.

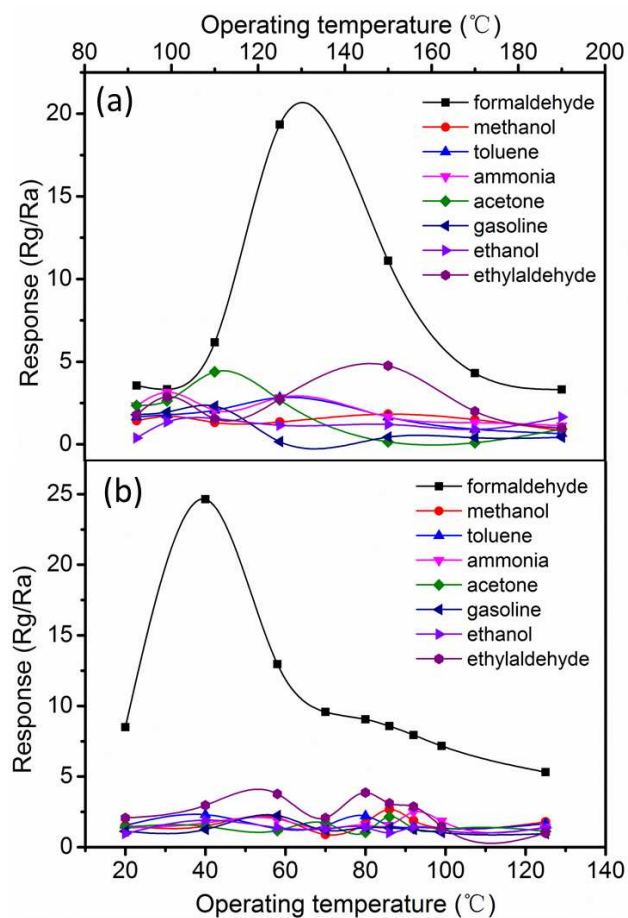


Fig. 6 Response-operating temperature curves for different tested gases of a) sensor based on Sample-B to 1 ppm gases and b) sensor based on Sample-C to 0.5 ppm gases.

Fig. 6 depicts the relationship between response and operating temperature of the as prepared sensors. The gas response β was defined as the ratio of the electrical resistance in gas (R_g) to that in air (R_a). To investigate the selectivity of the Sample-B and Sample-C, the response of formaldehyde, methanol, toluene, ammonia, acetone, gasoline, ethanol and ethylaldehyde were tested at different operating temperature respectively. It can be found that the sensor behaves well in selectivity to formaldehyde in Fig. 6. In Fig. 6a, the best response to 1 ppm formaldehyde based on Sample-B is 18.6 at 125 °C. To the other test gases, the highest response is lower than 4.0. In Fig. 6b, the best response to 0.5 ppm formaldehyde based on Sample-C is 24.5 at 40 °C. To the other test gases, the highest response is lower than 3.0. And Sample-C possesses a reasonable response to formaldehyde with even lower concentration and optimal operating temperature (40 °C) is 68% lower than that of Sample-B (125 °C). The mechanism behind this phenomenon can be discussed as follows: in the prepared Ag-LaFeO₃ sample, some Ag in the form of single matter as catalyzer mixes in the matrix. Some of them are filled between the grains of matrix to decrease the contact potential barrier and enhance the interfacial effect, which lead to lower resistance finally result in lower operating temperature. So after mixed with Ag-LaFeO₃, sample-C has lower operating temperature compared with sample-B.

The response and recovery times are defined as the time required reaching 90% response (recovery) when gas is in (out).²⁹ Fig. 7 presents a repetitive response-recovery characteristic for the two optimal sensors. As seen in Fig. 6a, the sensor based on Sample-B under a formaldehyde gas concentration range from 0.5 ppm to 20 ppm operated at 125 °C. The resistance of the sensor increases sharply when formaldehyde flow is in but returns to its original state while the gas flow is out although with some delay. When formaldehyde is in, the sensor begins to response which takes 90 s and when formaldehyde is out, the sensor begins to recover which takes 80 s. After the sensor has recovered about 90%, it became slower. The reason is when the concentration of formaldehyde on the surface of the materials is very low, the interaction between this part of formaldehyde and sensor is chemisorption;³⁰ it is very difficult for the formaldehyde to desorb from the surface.^{31, 32} The response and recovery time are about 90 s and 80 s, respectively. In Fig. 6b, the same conclusion can be draw that the response and recovery time based on Sample-C under a formaldehyde gas concentration range from 0.1 ppm to 20 ppm operated at 40 °C are 67 s and 104 s, respectively. It also can be found that the response increasing for Sample-B and Sample-C is near linear with the concentration of the formaldehyde (Also can be seen in ESI, Fig. S4). This is because there are a lot of formaldehyde-adsorbing vacancies on the surface of the sensor. When the concentration of test formaldehyde increases, the quantity of adsorbed formaldehyde on the surface of the sensor increases unceasingly, the electrons that the sensor got also increase gradually. Thus, for p-type semiconductors, the resistance value of the sensor also rises, eventually resulting in a response increase. At the same time, the response with formaldehyde concentration in a linear increase also shows that the sensor can be used to a continuous real-time monitoring at lower concentration of formaldehyde.

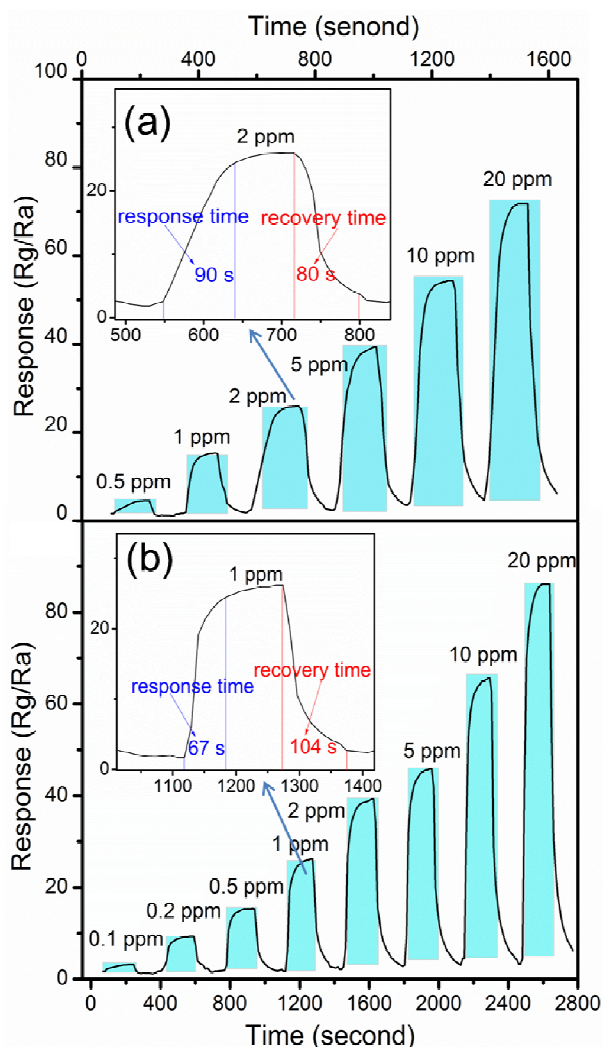


Fig. 7 Response-recovery time curve of the sensor based on a) Sample-B operated at 125 °C and b) Sample-C operated at 40 °C.

Conclusions

In summary, the selectivity of sensors can be improved using MIT. For the MINs, the optimal molar ratio of mol (template): mol (functional monomer) is $x = 1:3$. The structure of MINs is of orthogonal perovskite. The MINs with $x = 1:3$ has good selectivity for low concentration formaldehyde. To 1 ppm formaldehyde, the response is 18.6 at the operating temperature of 125 °C, and to the other test gases the response are all lower than 4.0, and the response time and recovery time are 90 s and 80 s, respectively. For the compounds, the optimal weight ratio of w (Sample-A): w (Sample-B) is $a:b = 9:1$. The structure of compounds is of orthogonal perovskite. The compound with $a:b = 9:1$ has good selectivity for low concentration formaldehyde. To 0.5 ppm formaldehyde, the response is 24.5 at the operating temperature of 40 °C, and to the other test gases the response are all lower than 3.0, and the response time and recovery time are

67 s and 104 s, respectively. To sum up, the compounds composed of Ag-LaFeO₃ and the MINs with a:b = 9:1 possess even better sensing properties to formaldehyde, and truly realized low limit of detection, low operating temperature, high response and high selectivity. These finding may present a new feasible way for exploring modified LaFeO₃ based on MIT sensing materials.

Acknowledgements

This work was supported by National Natural Science Foundation of China (No. 51402257), the Natural Science Foundation of Yunnan Province, China (NO. 2013FZ003).

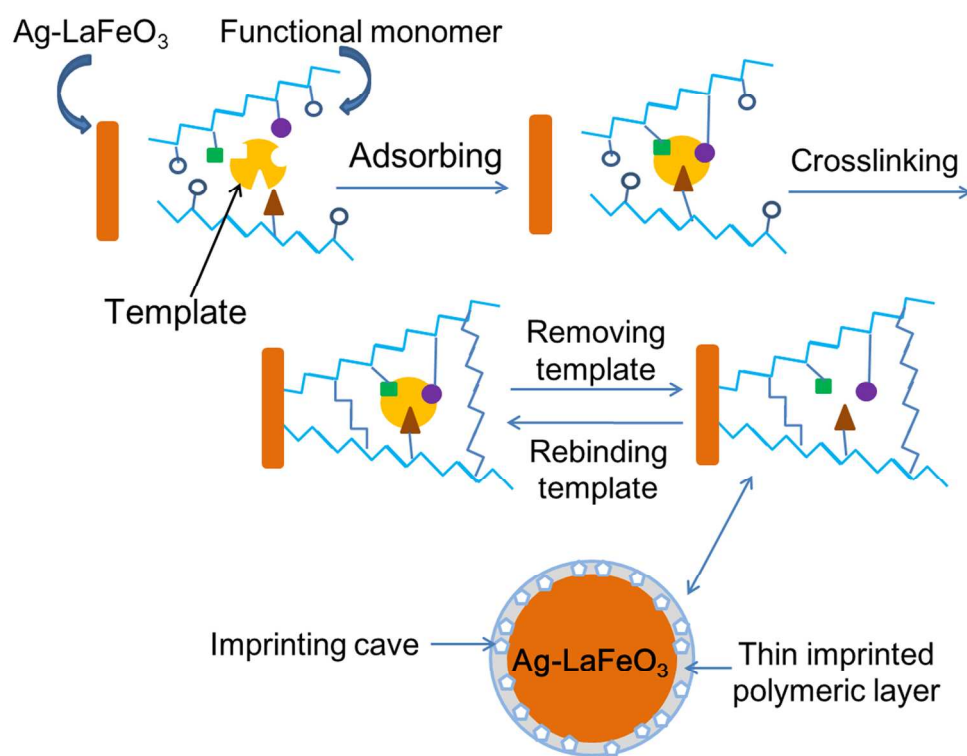
Notes and references

^aYunnan Key Laboratory for Micro/nano Materials & Technology, Yunnan University, 650091 Kunming, China. Email: qjliu@ynu.edu.cn

^bDepartment of Materials Science and Engineering, School of Physical Science and Technology, Yunnan University, 650091 Kunming, China

† Electronic Supplementary Information (ESI) available: The methods to measure gas response and four supporting figures. See DOI: 10.1039/c000000x/

- 1 J. H. Li, P. K. Dasgupta, W. Luke, *Anal. Chim. Acta* 2005, **531**, 51.
- 2 P. I. Palmer, D. J. Jacob, K. Chance, R. V. Martin, R. J. Spurr, T. P. Kurosu, I. Bey, R. Yantosca, A. Fiore, Q. Li, *Journal of Geophysical Research: Atmospheres (1984–2012)* 2001, **106**, 14539.
- 3 C. Yu, D. Crump, *Build. Environ.* 1998, **33**, 357.
- 4 J. H. Arts, M. A. Rennen, C. de Heer, *Regul. Toxicol. Pharm.* 2006, **44**, 144.
- 5 D. Belpomme, P. Irigaray, L. Hardell, R. Clapp, L. Montagnier, S. Epstein, A. J. Sasco, *Environ. Res.* 2007, **105**, 414.
- 6 N. Barsan, D. Koziej, U. Weimar, *Sens. Actuators, B* 2007, **121**, 18.
- 7 Y. D. Wang, I. Djerdj, M. Antonietti, B. Smarsly, *Small* 2008, **4**, 1656.
- 8 K. Wetchakun, T. Samerjai, N. Tamaekong, C. Liewhiran, C. Siri Wong, V. Kruefu, A. Wisitsoraat, A. Tuantranont, S. Phanichphant, *Sens. Actuators, B* 2011, **160**, 580.
- 9 M. M. Natile, A. Ponzoni, I. Concina, A. Glisenti, *Chem. Mater.* 2014, **26**, 1505-1513.
- 10 Y. M. Zhang, Y. T. Lin, J. L. Chen, J. Zhang, Z. Q. Zhu, Q. J. Liu, *Sens. Actuators, B* 2014, **190**, 171.
- 11 Y. M. Zhang, J. Zhang, J. L. Chen, Z. Q. Zhu, Q. J. Liu, *Sens. Actuators, B* 2014, **195**, 509.
- 12 K. Hirayama, Y. Sakai, K. Kameoka, K. Noda, R. Naganawa, *Sens. Actuators, B* 2002, **86**, 20.
- 13 A. Carlson, A. M. Bowen, Y. Huang, R. G. Nuzzo, J. A. Rogers, *Adv. Mater.* 2012, **24**, 5284.
- 14 F. L. Dickert, O. Hayden, *Adv. Mater.* 2000, **12**, 311.
- 15 G. Vlatakis, L. I. Andersson, R. Müller, K. Mosbach, 1993, **361**, 645.
- 16 G. Wulff, *Angewandte Chemie International Edition in English* 1995, **34**, 1812.
- 17 C. Pinel, P. Loisel, P. Gallezot, *Adv. Mater.* 1997, **9**, 582.
- 18 Y. Fuchs, O. Soppera, A. G. Mayes, K. Haupt, *Adv. Mater.* 2013, **25**, 566.
- 19 C. Zheng, X. L. Zhang, W. Liu, B. Liu, H. H. Yang, Z. A. Lin, G. N. Chen, *Adv. Mater.* 2013, **25**, 5922.
- 20 S. Vidyasankar, F. H. Arnold, *Curr. Opin. Biotech.* 1995, **6**, 218.
- 21 L. Xu, R. Q. Xing, J. Song, W. Xu, H. W. Song, *J. Mater. Chem. C* 2013, **1**, 2174.
- 22 B. Ding, X. F. Wang, J. Y. Yu, M. Wang, *J. Mater. Chem. C* 2011, **21**, 12784.
- 23 L. N. Han, D. J. Wang, J. B. Cui, L. P. Chen, T. F. Jiang, Y. H. Lin, *J. Mater. Chem. C* 2012, **22**, 12915.
- 24 B. Gao, J. Lu, Z. Chen, J. Guo, *Polymer* 2009, **50**, 3275.
- 25 M. Karlsson, A. Matic, P. Berastegui, L. Börjesson, *Solid State Ionics* 2005, **176**, 2971.
- 26 X. Cheng, K. Liang, G. Liu, N. Song, *Chemistry* 2007, **11**, 011.
- 27 Y. Kabbadj, T. Huet, D. Uy, T. Oka, *J. Mol. Spectrosc.* 1996, **175**, 277.
- 28 J. Yang, Y. Xu, S. Weng, F. Ye, H. Gao, J. Wu, *Spectrosc. Spectral Anal.* 2002, **22**, 741.
- 29 L. Mai, L. Xui, Q. Gaoi, C. Hani, B. Hui, Y. Pii, *Nano Lett.* 2010, **10**, 2604.
- 30 A. Bejaoui, J. Guerin, K. Aguir, *Sens. Actuators, B* 2013, **181**, 340.
- 31 S. Maric, J. Lörger, U. Herrmann, U. Schramm, J. Bargon, *Sens. Actuators, B* 2004, **101**, 265.
- 32 J. Zhou, Y. D. Gu, Y. F. Hu, W. J. Mai, P. H. Yeh, G. Bao, A. K. Sood, D. L. Polla, Z. L. Wang, *Appl. Phys. Lett.* 2009, **94**, 191103.



A novel formaldehyde gas sensor was developed for the first time using molecular imprinting technique to recognize small organic molecules.
158x122mm (300 x 300 DPI)